DIAGNOSIS OF ALKALI-SILICA REACTION IN AIRPORT PAVEMENT IN JAPAN

Naoya Kawamura[1*], Yuichiro Kawabata[2,3], Tetsuya Katayama[4]

[1] Airport Facilities Division, Airport Department, National Institute for Land and Infrastructure Management, Yokosuka, JAPAN

[2] Structural, Engineering Division, Port and Airport Research Institute, Yokosuka, JAPAN
[3] Université Paris-Est, IFSTTAR , Materials and Structures Department, Marne-la-Vallée, FRANCE

[4] Taiheiyo Consultant Co., Ltd., Sakura, JAPAN

Abstract

Petrographic examination and accelerated expansion tests were performed to clarify the causes of cracking due to alkali-silica reaction (ASR) in concrete pavement in a Japan airport. The deterioration was due to *pessimum* proportion effects caused by early-expansive ASR. ASR gel was observed in sand aggregates containing highly reactive minerals that exhibit *pessimum* proportion effects. Estimation of alkali contents in concrete confirmed the occurrence of ASR even when the total amount of alkali in the cement used was below 3.0 kg/m^3, which is the current regulated threshold for preventing ASR in Japan.

Two types of complementary test methods were also performed; one was a re-assessment of the structural performance of the affected pavement, and the other was an investigation of the relationship between the results of an expansion test and field behaviour. This study suggests that a falling weight deflectometer may be a promising tool for evaluating the performance of affected pavements, and that a modified expansion test to avoid alkali leaching can simulate slow expansion behaviours observed in the field.

Keywords: airport pavement, polarizing microscope, alkali contents, early-expansive ASR, accelerated expansion test

1 INTRODUCTION

Distress due to alkali-silica reaction (ASR) has rarely been reported in airport concrete pavement in Japan, even though pavement in airports in several other countries have shown ASR-distress related to the use of alkali-containing deicers [1]. A few years ago, ASR was identified in an airport in Japan where deicers had not been used. Considering that the pavement was exceeding its required service life, discussions took place on whether reconstruction or repair was required. It was decided that further evaluation was needed to determine the degree of ASR damage and potential for future expansion.

This paper presents the results of a study that identifies causes of cracking due to ASR and residual expansion of the pavement based on the application of a petrographic examination and accelerated concrete core expansion test. Based on the results, the validity of the preventive measures currently used in Japan is discussed. Moreover, two types of complementary tests were conducted. With respect to the re-assessment of current structural performance of the affected pavement, on-site test using a falling weight deflectometer (FWD) was performed. Then, a modified concrete expansion test able to avoid alkali leaching was performed in order to compare the test results with the expansive behaviour of field-exposure blocks extracted from the affected pavement. The validity of the tests is then discussed for further research.

2 OUTLINE OF THE PAVEMENT SITE

The concrete pavement investigated was constructed in a specific area of an airport nearly 20 years ago. It is a non-reinforced concrete pavement containing steel wire mesh (120 mm below the surface) and dowel bars (32 mm in diameter and 210 mm below the surface) linking two consecutive joints. Cracks were observed on the surface of about 40% of the pavement slabs, and most of the

* Correspondence to: kawamura-n92y2@mlit.go.jp

cracks could be observed on the corners. The pavement had not been subjected to freeze-thaw damage cycles or repeated loads by aircrafts. Even though aggregates used for the concrete were supplied from a plant at the same period, the extent of cracking varied among slabs. The cause of the cracks was investigated by comparing core samples taken from cracked slabs and sound ones.

3 DIAGNOSTIC PROCEDURES

3.1 Visual inspection of pavement surface

The surface of the pavement slabs was visually inspected to identify cracks and their patterns since the surface conditions varied among slabs.

3.2 Visual observation of concrete cores

Concrete cores (diameter 100mm, height 380mm) were taken from the pavement slabs, wrapped with plastic film and stored (over one or two days) to maintain their moisture content. The surface of the cores was then visually observed to identify whether reaction products or cracks were visible.

3.3 Polished thin section petrography

The severity of ASR was identified with a polarized microscope. Polished thin sections (25 mm × 35 mm, thickness 15 μm) were prepared from concrete cores taken from cracked and sound slabs. The sections were observed with polarizing microscopy to identify reacted rocks and minerals, the cracks and gel products around them, and the progress of reaction. The progress in each reacted rock type was categorized into five stages (Table 1): (1) the formation of reaction rims, (2) the exudation of ASR gel around the reacted aggregate, (3) the formation of gel-filled cracks within the reacted aggregate, (4) the propagation of gel-filled cracks from the reacted aggregate into the surrounding cement phase, and (5) the migration of ASR gel into air voids [2, 3].

The petrographic severity of ASR was rated, combining the above-mentioned reaction stages with the extent of damage (crack widths and frequency) in the section. The severity was defined as 1) slight, 2) moderate, and 3) severe. For example, the ASR severity of siliceous mudstone in the sound slab was higher than that of andesite in the cracked one (Table 1) since the extent of damage (cracks widths and frequency) in the mudstone was larger than that in the andesite, although the stage of ASR in both the andesite and the mudstone was stage four. These examinations were performed as in Katayama [2, 3].

3.4 Estimation of alkali contents in concrete

Following the method used by Katayama [2], alkali contents (Na_2O_{eq}) of the original concrete used in both the sound and cracked pavement were analytically estimated. The total alkali content of the concrete was calculated based on measurements of water-soluble alkali in the bulk concrete and separated coarse aggregate grains, and estimations of the minimum initial alkali content of the cement used in the concrete. The procedures used to calculate the contents are described as follows, with additional details described in the references [2, 3].

After the cores were separated into coarse aggregate and mortar, their water-soluble alkali was extracted with the General Project Method [4]: temperature: 40 ºC, duration: 0.5 h, and liquid/solid = 10.

The minimum initial amount of cement alkali (Na_2O_{eq}), exclusive of water-soluble alkali sulfates, was estimated by a quantitative energy-dispersive X-ray spectroscopy (EDS) analysis (15 kV, mainly 0.12 nA) of unhydrated cement clinker phases found in the polished thin sections. The minimum amount of cement alkali was converted to total cement alkali content with a correction factor for the missing alkali of alkali sulfates. The amount of water-soluble alkali from cement was calculated from the total cement alkali content with a correction factor of 0.6. The total available alkali in the concrete was calculated as the sum of the total cement alkali and water-soluble alkali from coarse and fine aggregates plus alkalis derived from chemical admixtures and environment.

3.5 Accelerated concrete core expansion test

One core was taken from both a sound slab and a cracked one, and they were cut so as to attach belts with measuring studs (diameter 50 mm, length 130 mm, span 100 mm). Then, they were subjected to an expansion test as described by Katayama [4]. In this test, the cores were immersed in NaOH solution (80 ºC 1 M) and the expansions were measured for 28 days. This method was used to detect potential further reactivity of aggregate in the concrete.

4 RESULTS AND DISCUSSION

4.1 Visual inspection of pavement surface

Figures 1–3 show pavement surfaces in the survey area. Figure 1 shows the apparently sound slabs: cracks were not found on the surface. Figures 2–3 show cracks in the corners of the deteriorated slabs. Some cracks were only found at the corners of the slabs (Figure 2), and others propagated along the slab joint from the corner, which is commonly termed D-cracking (Figure 3). The extent of cracking differed in every adjacent slab. These results suggest that the extent of degradation differed from one slab to another. Figure 4 shows a close-up view of the pavement surface. Reaction products from cracks and pop-outs of concrete were also found.

4.2 Visual inspection of core

Figures 5–6 show cores taken from a sound pavement slab and a cracked one, respectively. Cracks could not be detected on the lateral surface of the core taken from the sound slab (Figure 5(a)), but ASR gel and reaction rims were verified around fine aggregates located on the lateral surface (Figure 5(b)). On the other hand, cracks were easily found in the bulk of the cores taken from the cracked slab (Figure 6(a)). The macrocracks were mainly horizontal and found at depths where both the steel wire mesh and dowel bars were located. The lower part of the core did not retain its original shape because of a high degree of damage. ASR gel, reaction rims, and pop-outs were found on the lateral surface (Figure 6(b)). ASR occurred in both sound and cracked slabs because the reaction products detected on both slabs have ASR-specific characteristics.

4.3 Polished thin section petrography

Table 1 summarizes rock types comprising coarse and fine aggregates, a range of mineral types, the progress of ASR, and the severity of ASR for thin sections prepared from the cores taken from the sound and the cracked slabs.

Sound pavement slab

Coarse aggregates are mainly composed of crushed chert and partially contained sandstone. Fine aggregates are pit sands composed of volcanic rocks, mudstone and minerals derived from volcanic rocks. ASR was identified in tuffaceous sandstone, siliceous mudstone and radiolarian siliceous mudstone containing opal. These aggregates produced concentric cracks inside the reaction rim and radial cracks extending into the surrounding cement paste as shown in Figure 7. These cracks were filled with ASR gel.

Cracked pavement slab

Coarse and fine aggregates in the cracked slab were identified as being the same as the ones found in the sound slab, but the content ratio of chert in the cracked slab was higher than that in the sound one. Besides the amount of fine aggregate with ASR, the extent of ASR in the cracked slab was larger than that in the sound slab. ASR was identified in volcanic rocks such as andesite, altered andesite and glassy rhyolite. In addition, ASR was identified in mudstone, radiolarian siliceous mudstone, calcareous mudstone and tuffaceous sandstone. Pop-outs were detected in the mudstones and sandstone.

Figure 8A shows a reaction rim around glassy rhyolite, which is due to its reaction with volcanic glass. Cracks filled with ASR gel propagated into the cement paste from the aggregate particles. These cracks were parallel to the direction of the horizontal macrocracks in the concrete core. Carbonation was identified in the cement paste around the cracks, which was due to repeated infiltration and drying of rain water.

Figure 8B shows a radiolarian siliceous mudstone. ASR was identified in opal contained in the mudstone. Concentric cracks inside the reaction rim and radial cracks extending into the surrounding cement paste were also detected. The expansion cracks and adjacent air voids were filled with ASR gel.

4.4 Alkali Contents in Concrete

Table 2 shows the minimum and total amounts of cement alkali, water-soluble alkali, and total available alkali in the sound and cracked slabs. Total available alkali was the summation of the total cement alkali and water-soluble alkali of the coarse and fine aggregates, and alkalis from the other sources (chemical admixture and environment). Total amounts of cement alkali in the sound and cracked slabs were Na_2Oeq 2.3 kg/m^3 and Na_2Oeq 2.5 kg/m^3, respectively, which represents a small difference in the respective total amounts of cement alkali. The water-soluble alkali of the aggregates (plus alkalis derived from chemical admixtures and environment) corresponded to Na_2Oeq 0.5–0.7

kg/m^3. Thus, the total amount of available alkali in the sound and cracked slabs were Na_2Oeq 2.8 kg/m^3 and Na_2Oeq 3.2 kg/m^3, respectively. The amount of total available alkali in the cracked slab was higher than that in the sound one.

4.5 Accelerated concrete core expansion test

Figure 9 shows the results of the accelerated concrete core expansion test using a NaOH solution. After 21 days, concrete cores taken from the cracked and sound slabs showed expansions of 0.12% and 0.11%, respectively. Both cores exceeded the deleterious limit in this test (0.10% at 21 days [2]). This suggests that both types of pavement slabs still contain large amounts of reactive minerals, and hence, have high potential for producing expansion.

4.6 Diagnosis of ASR in the airport pavement

Cause of pavement deterioration

ASR was identified in fine aggregates containing rhyolite with volcanic glass and mudstone with opal. Opal is a highly reactive silica mineral causing early-expansive ASR with a small *pessimum* proportion (<5 wt.%, [5]). This suggests that the cause of pavement deterioration is early-expansive ASR due to the reactive aggregates that exhibit a *pessimum* proportion effect. This study confirmed ASR occurrence even when the total amount of cement alkali in the concrete (2.3 kg/m^3) was lower than 3.0 kg/m^3, which is the currently regulated alkali threshold for preventing ASR in Japan.

Since the initial amount of cement alkali differed slightly among slabs, the alkali amount in the cement varied depending on the cement lot. Furthermore, the amount of reactive minerals contained within the fine aggregates also can vary. These variations contributed to ASR occurrence with different degrees of cracking among the slabs. In particular, slight differences in the amount of reactive minerals can greatly affect ASR occurrence and progress since ASR-affected concrete containing opal presented a small *pessimum* proportion.

These discussions were based on the petrographic examination as in Katayama [2]. This suggests that the sophisticated examination was an essential step in providing a proper diagnosis of the ASR-affected pavement.

Potential residual expansion

There is a possibility that expansion and cracking occur on the surface of sound pavement slabs because the concrete still has a high potential to produce residual expansion.

4.7 Preventive measures

To prevent ASR in airport pavements in Japan, the threshold of total alkali amount in concrete is discussed. The total amounts of cement alkali in the sound and cracked slabs were Na_2Oeq 2.3 kg/m^3 and Na_2Oeq 2.5 kg/m^3, respectively. Since ASR was identified in the sound and cracked slabs, the total amount of cement alkali of 3.0 kg/m^3, which is the currently regulated alkali threshold for preventing ASR in Japan, was insufficient to prevent ASR in airport pavement, especially if the concrete presents reactive aggregates exhibiting a *pessimum* effect. The result points to the necessity of re-considering the threshold amount of alkali in concrete.

5 COMPLEMENTARY TESTING A: RE-ASSESSMENT OF THE PAVEMENT AFFECTED

5.1 FWD test

Assessing the current structural performance of ASR-affected pavement is one concern when judging whether pavements should be repaired. FWD (shown in Figure 10) is commonly used as a non-destructive test procedure for analysing the load-bearing capacity of pavements. This test consists of a trailer-mounted device that operates by dropping a weight on to the pavement and measuring the resulting pavement deflections. An FWD test can be a promising way to evaluate the integrity of the pavement under examination, but there were few opportunities to apply the test method to the affected pavement. Therefore, the test was performed on the corner of the cracked and the sound slabs in order to demonstrate applicability of the test for integrity evaluation of the affected pavement. The load used for the FWD was 150 kN: this load was applied to the pavement through a circular loading plate (diameter 300 mm) and surface deflection was measured at the centre of the plate.

5.2 Result

Figure 11 shows an example of the test results. Deflections of sound slabs were around 0.2 mm, whereas those of cracked slabs were approximately twice as large. The increase in the deflection

is due to cracks and resultant loss of stiffness. Reduction in stiffness raises some serious concerns in terms of serviceability and safety of airport facilities. An FWD test can track the stiffness indirectly, and hence is a promising tool for evaluating the integrity of ASR-affected pavement, although further research is still necessary.

6 COMPLEMENTARY TESTING B: RELATIONSHIP BETWEEN ACCELERATED EXPANSION TEST AND FIELD EXPANSION

6.1 Outline

For management of ASR-affected pavement, predicting expansion and consequent performance degradation is essential. FWD can detect current performance, but there is no way to estimate performance in the future. This situation foregrounds the necessity to predict possible expansion and the resultant deformation and damage. Although some numerical tools have been developed [6, 7], the procedure of expansion tests designed to identify material properties has some critical problems. One of the problems is alkali leaching. In this regard, the second author of the present paper proposed a method to estimate the expansion attained in the field using results of accelerated expansion tests in which the concrete specimens were wrapped with wet cloth containing an alkali solution [8]. The method of wrapping concrete with wet cloth containing an alkaline solution was proposed as a curing method to avoid the leaching, and its effectiveness has been demonstrated [9].

Complementary tests were performed to investigate applicability of the expansion test. First, field exposure tests of the concrete blocks cut from the airport pavement slab were performed. Accelerated expansion tests were also performed using cores taken from the concrete blocks.

6.2 Materials and methods

Field exposure test

Field exposure tests were performed on five concrete blocks (1000 mm × 1000 mm × 380 mm) that were cut from the airport pavement slabs investigated in this study. The blocks were called B1, B2, B3, B4, and B5 in order of their level of cracking. The slab from which B1 was taken suffered severe D-cracking (Figure 12), whereas the one from which B5 was taken presented a slight reaction but no apparent cracking. After cutting, the blocks were moved to the Port and Airport Research Institute (PARI) and stored outdoors (Figure 13). To measure expansion of the blocks, the blocks were fitted with stainless steel pins glued on to the upper surface (span 200 mm); these pins were used as measurement bases to set a digital extensometer.

Accelerated expansion test

Accelerated expansion tests were performed on one concrete cores each (diameter 100mm, height 380 mm) taken from B2 and B5 approximately two years after starting the field exposure test. The cores were equipped with stainless steel pins glued on the lateral sides (span 100 mm, 50 mm pitch). They were wrapped with two wet papers containing 50 g of 1.5 M NaOH, following the so-called alkali-wrapping protocol. After being covered by thin plastic film and stored in a thick plastic bag to prevent moisture movement between cores and chamber, the specimens were stored in a chamber with the temperature controlled at 38 ºC.

6.3 Results

Figure 14 shows the expansion of blocks B2 and B5 for comparison with the results of the accelerated expansion test. The expansion illustrated in the graph is the expansion strain of each block. The expansions of both blocks B2 and B5 block were approximately 0.025% at 5 months. The expansion values at early stages (up to 5 months) may be attributed to recovered creep strain due to the release of restraint in the pavement. Hydric recovery of water was not likely to contribute to the expansions since water was sufficiently supplied to the blocks when they were cut and moved to this site. After 5 months, the expansion of B2 was larger than that of B5.

The expansion of the cores of B2 and B5 are shown in Figure 15. The expansion illustrated in the graph is the summation of expansions between adjacent steel pins glued on to the vertical direction of a core. The expansion of the core of B2 was the same as that of B5 from week one until week six. After six weeks, B2's core expanded more than B5's. The expansion test using the alkali-wrapping protocol can simulate the slow expansion behaviour shown in the field, which suggests that the protocol can contribute to improvement of the prediction of expansion. For future research, the prediction of expansion using the modified expansion test will be performed and will be compared to expansion in the field exposure test. The applicability of the modified test will then be validated.

7 CONCLUSIONS

Petrographic examination and accelerated concrete core expansion tests were performed to clarify causes of cracking due to ASR and investigate the potential of residual expansion of concrete pavement in a Japanese airport. In addition, two types of complementary tests were conducted; first, the re-assessment of the current structural performance of the affected pavement was performed and second, an investigation of the relationship between the accelerated results and field behaviour was analysed. The following conclusions can be drawn:

1) The petrographic examination suggested that the cause of pavement deterioration was early-expansive ASR due to the presence of reactive fine aggregates containing volcanic glass and opal, exhibiting a *pessimum* proportion effect.

2) Estimation of alkali content in the concrete suggested that the total amount of cement alkali was Na_2Oeq 2.5 kg/m^3 in the cracked slab and Na_2Oeq 2.3 kg/m^3 in the sound slab. ASR occurred even when the total amount of cement alkali in the concrete was lower than 3.0 kg/m^3, which is the currently regulated alkali content threshold for causing ASR in Japan.

3) There is a possibility that cracking will occur on the surface of sound pavement slabs in the future. This is due to the slabs' high potential for residual expansion, as demonstrated by the results of the accelerated expansion tests.

4) FWD testing can indirectly track the stiffness of ASR-affected pavement, and hence can be a promising tool for evaluating the integrity of affected pavement.

5) The expansion test with the alkali-wrapping protocol can simulate the slow expansion behaviour shown in the field, especially during the final expansion levels. This suggests that the protocol can contribute to improving the prediction of expansion.

8 REFERENCES

[1] Shi, X. (2008): Impact of Airport Pavement Deicing Products on Aircraft and Airfield Infrastructure, ACRP Synthesis 6, Airport Cooperative Research Program, Transportation Research Board, National Academies.

[2] Katayama T, Tagami M, Sarai Y, Izumi S and Hira T (2004): Alkali-aggregate reaction under influence of deicing salts in the Hokuriku district, Japan, Materials Characterization, vol.53, pp 105-122.

[3] Katayama T, Oshiro T, Sarai Y, Zaha K, and Yamato T (2008): Late-expansive ASR due to imported sand and local aggregates in Okinawa, southwestern Japan, 13th ICAAR, Trondheim, Norway, pp.862-873.

[4] General Project Method (1989): Analysis of water-soluble alkali in concrete. Development of technology to improve durability of concrete structures. Japan: Ministry of Construction, pp159-160.

[5] Katayama, T., Helgason, T. S. and Olafsson, H (1996): Petrography and alkali-reactivity of some volcanic aggregates from Iceland, 10th ICAAR, Melbourne, Australia, pp377-384.

[6] Seignol JF., Baghdadi N, and Toutlemonde F (2009): A macroscopic chemo-mechanical model aimed at re-assessment of delayed-ettringite-formation affected concrete structures, Proceedings of the 1st International Conference on Computational Techniques in Concrete Structures.

[7] Saouma V, Perotti L, and Shimpo T (2007): Stress analysis of concrete structures subjected to alkali-aggregate reactions, ACI Structural Journal, No. 104, pp. 532-541.

[8] Kawabata Y, Yamada K, Ogawa S, and Sagawa Y (2014): Simplified prediction of ASR expansion of concrete based on accelerated concrete prism test, Cement science and concrete technology, Vol. 67, pp449-455.

[9] Yamada K, Karasuda S, Ogawa S, Osako M, Hamada H, and Isneini M, (2014): CPT as an evaluation method of concrete mixture for ASR expansion, Construction and Building Materials, Vol. 33, No.6, pp. 69-79.

TABLE 1: Severity of ASR between sound and cracked slabs with reference to the reacted rock type of the aggregate in concrete as determined by thin section petrography.

	Rock types		Progress of ASR →					Severity of ASR
			(1)	(2)	(3)	(4)	(5)	
			Aggregate			Cement paste		Petro-
			Rim	Gel-rim	Gell-filled crack		Gel-void	graphic
Sound pavement slab	C	Chert	(x)					1
	F	Andesite		x				1
		Dacite	x					1
		Rhyolitic welded tuff	x					1
		Siliceous mudstone	(x)		x+	x		3
		Radiolarian siliceous mudstone	(x)		xx+	xx	x	3
		Tuffaceous sand stone	(x)		x+	x	x	3
		Radiolarian chert	(x)					1
		Chert	x					1
	Overall rating							2
Cracked pavement slab	C	Chert	(x)		(x)			1
	F	Andesite	x	(x)	x	x		2
		Altered andesite		(x)	x	x	x	3
		Dacite	xx	xx				1
		Glassy rhyolite	xx	x	x	x	x	3
		Rhyolite	x	x				1
		Rhyolitic welded tuff	x					1
		Tuff	x		xx+	xx	x	3
		Tuffaceous mudstone			xx+	xx		3
		Mudstone	(x)	(x)	x+	x	x	3
		Calcareous mudstone	x		xx+	xx	x	3
		Radiolarian siliceous mudstone	(x)		xx+	xx	x	3
		Chert	x	x	(x)			1
	Overall rating							3

C: coarse aggregate, F: fine aggregate, Blue coloured cells indicate volcanic rock or volcanogenic sedimentary rock

Intensity of ASR : xx: conspicuous, x: common, (x): rare, +: pop-out

Petrographic severity of ASR: 1) slight, 2) moderate, 3) severe

TABLE 2: Alkali contents of concrete as estimated from EDS analysis of unhydrated cement and wet chemical analysis of water-soluble alkali of concrete and separated coarse aggregate.

	Clinker			Cement		Coarse aggregate (extr.)			Others	Concrete			
	Minimum alkali by EDS			Total alkali	Water-sol. alk	Water-soluble alkali			Total alkali	Water-soluble alkali			Total alkali
	measured			estimated		measured			est.	measured			est.
	%			Na_2Oeq kg/m^3		%		Na_2Oeq kg/m^3		%		Na_2Oeq kg/m^3	
	Na_2O	K_2O	(1)	(2)	(3)	Na_2O	K_2O	(4)	(5)	Na_2O	K_2O	(6)	(7)
1	0.43	0.21	0.56	2.28	1.37	0.02	0.03	0.44	0.03	0.05	0.04	1.84	2.75
2	0.42	0.29	0.61	2.49	1.49	0.03	0.03	0.54	0.13	0.06	0.05	2.16	3.16

1 Core taken from sound pavement slab, 2 Core taken from cracked pavement slab

(1): $Na_2Oeq = Na_2O + 0.658K_2O$

(2): 1.2 x ((1)/100) x 340 kg/m^3

(3): 0.6 x (2), 0.6 = water-soluble alkali ratio

(4): Measured General Project Method by water-soluble alkali of separated coarse aggregate, including absorbed alkali from cement paste

(5): Water-soluble alkali of fine aggregate plus the alkali from the other sources = (6) - (3) -(4)

(6): Measured by General Project Method

(7): Total available alkali of concrete = (2) + (4) + (5) = (2) + (6) - (3)

Total available alkali from coarse and fine aggregate plus the alkali from the other sources = (4) + (5) = (6) -(3)

FIGURE 1: Sound concrete slab

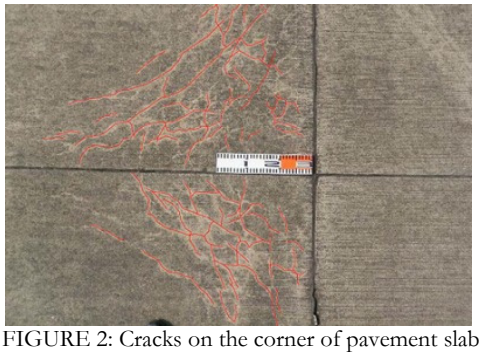

FIGURE 2: Cracks on the corner of pavement slab

FIGURE 3: Cracks propagated along the slab joint

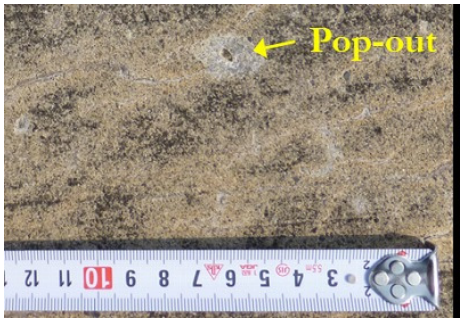

FIGURE 4: Close-up view of the crack

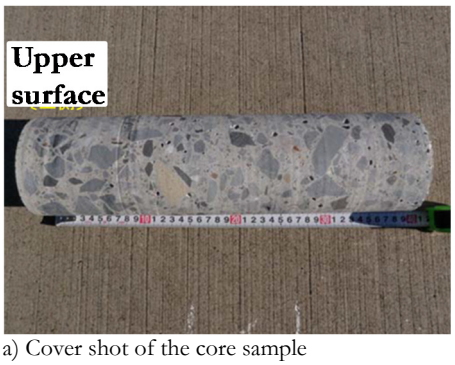

a) Cover shot of the core sample

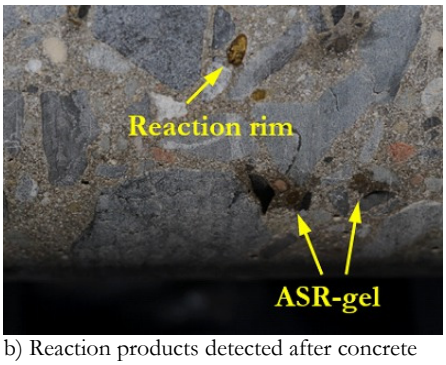

b) Reaction products detected after concrete was wrapped with plastic film for one day

FIGURE 5: Core taken from the sound slab

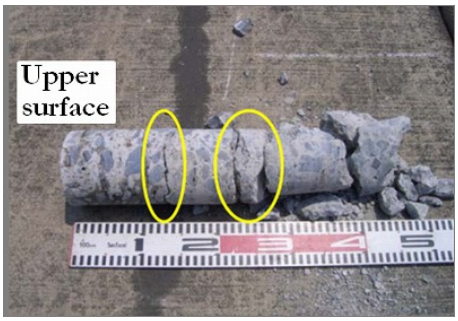

a) Cover shot of the core sample

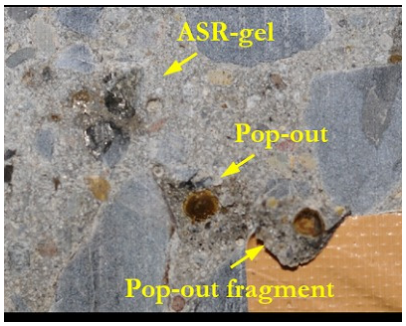

b) Reaction products detected after concrete was wrapped with plastic film for one day

FIGURE 6: Core taken from the cracked slab

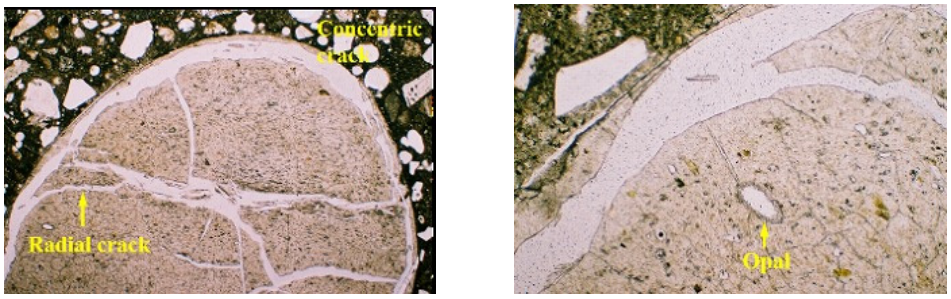

FIGURE 7: Radiolarian siliceous mudstone identified in a core taken from the sound slab

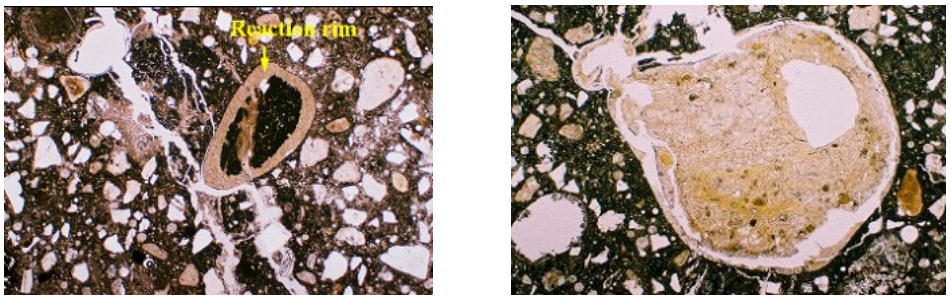

a) Glassy rhyolite b) Radiolarian siliceous mudstone

FIGURE 8: Polished thin section of a core taken from the cracked slab

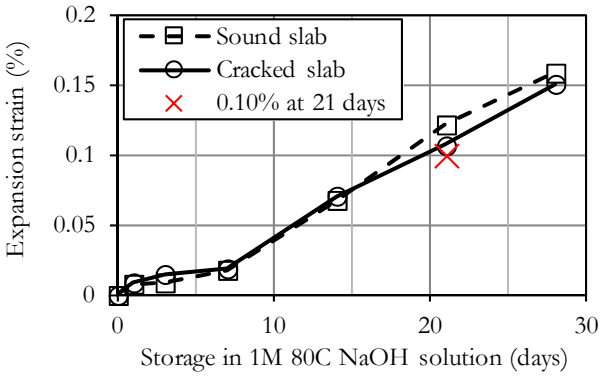

FIGURE 9: Accelerated concrete core expansion test using NaOH solution

FIGURE 10: Falling weight deflectometer

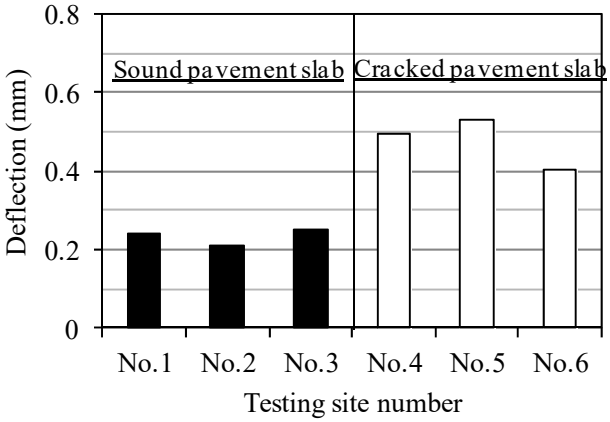

FIGURE 11: Results of falling weight deflectometer test on the corner of cracked and sound slabs

FIGURE 12: Slab where B1 was taken (red frame in the image is the cutting position)

FIGURE 13: Exposure block

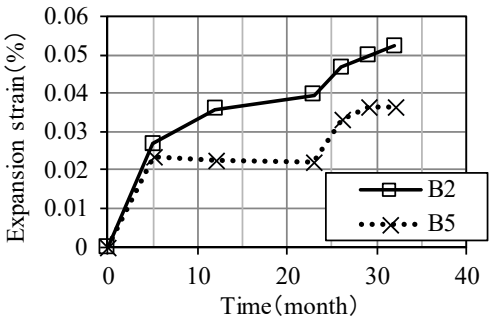

FIGURE 14 Expansion of blocks

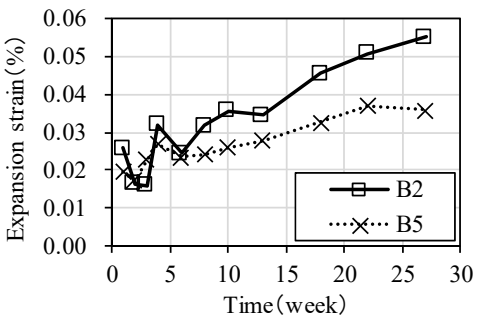

FIGURE 15 Expansion of cores